Sustained Oscillation Analysis of VSC Considering High-Order Oscillation Components

Yuzhi Wang, Liang Wang, and Qirong Jiang

***Abstract*—Oscillations of grid-connected voltage source converter (VSC) usually reaches sustained state because of the limiters in controller. Describing function has been adopted to analyze the amplitude and frequency of the sustained oscillations, but high-order oscillation components caused by the limiter are ignored in previous literatures. This letter proposes an analysis method for sustained oscillations which considers high-order oscillation components. This method could obtain a more precise oscillation frequency and the amplitude of 1st, 2nd, and 3rd order components. The proposed method is verified by case studies and simulations in PSCAD/EMTDC.**

***Index Terms*—Voltage source converter, sustained oscillation, controller limiter, high-order components, describing function.**

I. Introduction

ELECTROMAGNETIC oscillations caused by the interaction between VSCs and AC grid could be studied based on small-signal analysis method, such as eigenvalue analysis and impedance analysis [1]. However, the oscillations cannot diverge continuously due to limiters in the controller of VSC and sustained oscillations finally appear, which cannot be analyzed by small-signal methods. Hence, describing function has been adopted to model the limiter and analyze the sustained oscillations in previous literatures [2], [3].

When oscillation occurs, there are usually multiple oscillation components in the system, which are produced by the nonlinear parts of VSC [4], [5]. When the dominant 1st order oscillation component goes through the nonlinear parts, such as PLL, limiters and so on, high-order components could be generated. According to the existing literatures, the high order components are ignored and only 1st order component is considered in the analysis process. However, the proportion of high order components increase remarkably when severe oscillation happens and the precision of existing describing function method will be obviously reduced.

Manuscript received July 21, 2021; revised October 27, 2021 and January 16, 2022; accepted February 24, 2022. Date of publication March 7, 2022; date of current version April 19, 2022. This work was supported in part by the National Natural Science Foundation of China under Grant U1866601. Paper no. PESL-00179-2021. *(Corresponding author: Qirong Jiang.)*

Yuzhi Wang and Qirong Jiang are with the Department of Electrical Engineering, Tsinghua University, Beijing 100084, China (e-mail: yzyz13@163.com; qrjiang@mail.tsinghua.edu.cn).

Liang Wang is with the School of Automation, Beijing Institute of Technology, Beijing 100081, China (e-mail: s.wl@live.cn).

Color versions of one or more figures in this article are available at https://doi.org/10.1109/TPWRS.2022.3156431.

Digital Object Identifier 10.1109/TPWRS.2022.3156431

To address this issue, this letter proposes an analysis method for sustained oscillations which considers high-order oscillation components. We improved the traditional describing function method and proposed an improved describing function of asymmetric limitation considering 2nd and 3rd order oscillation components. This proposed method could obtain more precise results of oscillation frequency and amplitude than the traditional method. The amplitude of 2nd and 3rd order oscillation components could also be calculated out.

II. The Improved Describing Function Considering High-Order Components

A. Traditional Describing Function Method

Describing function method has been adopted to model nonlinear element. It is assumed that the input of the nonlinear element is a sinusoidal signal $x(t) = A\sin\omega t$. So the output $h(x)$ can be decomposed into a Fourier series with a fundamental frequency $f = \omega/2\pi$. The describing function $N(A)$ is defined as the ratio of the 1st order output Fourier series to the input:

$$N(A) = \frac{\int_0^{2\pi} h(x)\sin\omega t\ d\omega t + j\int_0^{2\pi} h(x)\cos\omega t\ d\omega t}{A\pi} \triangleq \frac{a_1 + jb_1}{A} \tag{1}$$

Hence, the nonlinear element can be approximated as a variable gain correlated to the input signal. The above method has been applied to the analysis of 1st order oscillation components in previous research.

B. Describing Function Considering High-Order Components

The operating point of VSC is variable, so symmetrical limitation rarely appears. Asymmetric limitation is the most common case. Here, take unilateral limitation as an example, shown in Fig. 1, in which $\phi_1 = \arcsin(\delta_1/A)$ and $\phi_2 = \pi - \phi_1$.

According to (1), the traditional describing function of the unilateral limitation can be denoted as $N_1(A)$ and there is

$$\begin{cases} a_1 = \frac{1}{\pi}\left[\int_0^{\phi_1} x(t)\sin\omega t\ d\omega t + \int_{\phi_1}^{\pi-\phi_1} \delta_1\sin\omega t\ d\omega t \right. \\ \qquad \left. + \int_{\pi-\phi_1}^{2\pi} x(t)\sin\omega t\ d\omega t)\right] \\ b_1 = \frac{1}{\pi}\left[\int_0^{\phi_1} x(t)\cos\omega t\ d\omega t + \int_{\phi_1}^{\pi-\phi_1} \delta_1\cos\omega t\ d\omega t \right. \\ \qquad \left. + \int_{\pi-\phi_1}^{2\pi} x(t)\cos\omega t\ d\omega t\right] = 0 \end{cases} \tag{2}$$

Therefore, when a single sinusoidal signal goes through the limiter, there is no phase shift between the input and the 1st order

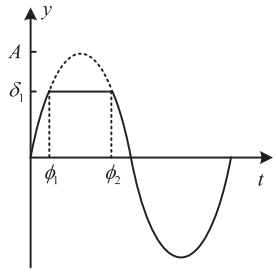

Fig. 1. Sinusoidal signal with unilateral limitation.

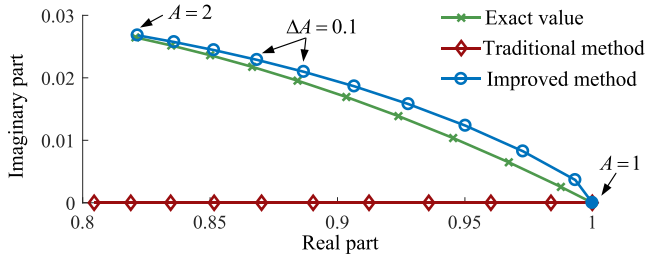

Fig. 2. Calculation results of the describing function.

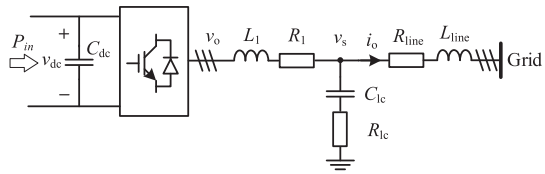

Fig. 3. Structure of the grid-connected VSC.

output Fourier series. However, when oscillation happens, high-order components could be found in both inputs and outputs. When there are many components of different frequencies in the input signal of a limiter, we cannot get an analytical solution of the describing function. So, an approximate calculation method is proposed for the describing function, which considers 2nd and 3rd order components. Supposing the input signal is

$$\begin{aligned} x'(t) &= A\sin\omega t + A_2\sin(2\omega t+\alpha_2) + A_3\sin(3\omega t+\alpha_3) \\ &\triangleq x(t) + \Delta x(t) \end{aligned} \tag{3}$$

Obviously, the frequency of $x'(t)$, which is denoted by f_s, is equal to $\omega/2\pi$. The output of the unilateral limiter is a signal with the same period. Therefore, the output signal only contains harmonics of nf_s (n is an arbitrary positive integer). Because the system is closed-loop, the input and output signal of the limiter have the same spectrum when sustained oscillation happens. Therefore, the effect of the limiter on the input signal can be analyzed by Fourier Series. When $x'(t)$ goes through the unilateral limiter, we have

$$\begin{cases} a_1' = \frac{1}{\pi}\left[\int_0^{\phi_1'} x'(t)\sin\omega t\, d\omega t + \int_{\phi_1'}^{\phi_2'} \delta_1 \sin\omega t\, d\omega t \right. \\ \qquad\qquad \left. + \int_{\phi_2'}^{2\pi} x'(t)\sin\omega t\, d\omega t\right] \\ b_1' = \frac{1}{\pi}\left[\int_0^{\phi_1'} x'(t)\cos\omega t\, d\omega t + \int_{\phi_1'}^{\phi_2'} \delta_1 \cos\omega t\, d\omega t \right. \\ \qquad\qquad \left. + \int_{\phi_2'}^{2\pi} x'(t)\cos\omega t\, d\omega t\right] \end{cases} \tag{4}$$

Precise value of ϕ_1' and ϕ_2' can be obtained by solving transcendental equation or by numerical calculation, which is too complex to be adopted in analysis. Equation (4) could be further written as (5), in which ξ_1 and ξ_2 are the angle error introduced by the 2nd and 3rd order components.

$$\begin{cases} a_1' = \frac{1}{\pi}\left[\int_0^{\phi_1+\xi_1} x'(t)\sin\omega t\, d\omega t + \int_{\phi_1+\xi_1}^{\pi-\phi_1+\xi_2} \delta_1 \sin\omega t\, d\omega t \right. \\ \qquad\qquad \left. + \int_{\pi-\phi_1+\xi_2}^{2\pi} x'(t)\sin\omega t\, d\omega t\right] \\ b_1' = \frac{1}{\pi}\left[\int_0^{\phi_1+\xi_1} x'(t)\cos\omega t\, d\omega t + \int_{\phi_1+\xi_1}^{\pi-\phi_1+\xi_2} \delta_1 \cos\omega t\, d\omega t \right. \\ \qquad\qquad \left. + \int_{\pi-\phi_1+\xi_2}^{2\pi} x'(t)\cos\omega t\, d\omega t\right] \end{cases} \tag{5}$$

In practical oscillation cases, because 2nd and 3rd order components are generated by 1st order components, A_2 and A_3 are relatively smaller than A. So, ξ_1 and ξ_2 are close to zero. Hence, simplification is made that $\phi_1' \doteq \phi_1$ and $\phi_2' \doteq \pi - \phi_1$. Therefore, the improved describing function considering 2nd and 3rd order components is

$$\begin{aligned} N_1'(A, A_2, A_3, \alpha_2, \alpha_3) &= \frac{1}{A}(a_1' + jb_1') \\ &= N_{11}(A) + N_{12}(A, A_2, \alpha_2) + N_{13}(A, A_3, \alpha_3) \end{aligned} \tag{6}$$

In which

$$\begin{cases} N_{11}(A) = N_1(A) = \frac{1}{\pi}\left(\arcsin(\frac{\delta_1}{A}) + \frac{\delta_1}{A}\sqrt{1-(\frac{\delta_1}{A})^2} + \frac{\pi}{2}\right) \\ N_{12} = \frac{1}{\pi}\frac{4A_2}{3A}\sin\alpha_2\sqrt{1-(\frac{\delta_1}{A})^2}\left(\frac{1}{2}+(\frac{\delta_1}{A})^2\right) \\ \qquad - \frac{j}{\pi}\frac{4A_2}{3A}\cos\alpha_2\sqrt{1-(\frac{\delta_1}{A})^2}\left(1-(\frac{\delta_1}{A})^2\right) \\ N_{13} = \frac{1}{\pi}\frac{2A_3}{A}(\frac{\delta_1}{A})^3\cos\alpha_3\sqrt{1-(\frac{\delta_1}{A})^2} \\ \qquad + \frac{j}{\pi}\frac{2A_3}{A}\frac{\delta_1}{A}\sin\alpha_3\left(\sqrt{1-(\frac{\delta_1}{A})^2}\right)^3 \end{cases} \tag{7}$$

It is clear that the improved describing function is a variable complex gain when high-order components are taken into consideration, which lead to a phase shift in 1st order output.

Fig. 2 shows the calculation results of a describing function of the limiter. In this case, $\delta_1 = 1$ and the ratios of 2nd and 3rd order components to 1st order component keep unchanged ($A_2 = 0.1A$, $A_3 = 0.05A$). The phases of 2nd and 3rd order components are both $3\pi/4$. The amplitude of 1st order component varies from 1 to 2. Compared to the traditional method, the proposed method has a better precision.

Similarly, the output 2nd and 3rd order components can also be calculated and the describing functions of these components are defined as the ratio of the 2nd/3rd order output components to the 2nd/3rd order input, denoted as $N_2'(A,A_2,A_3,\alpha_2,\alpha_3)$ and $N_3'(A,A_2,A_3,\alpha_2,\alpha_3)$.

III. Analysis Model of Sustained Oscillations

The structure of the grid-connected VSC system is presented in Fig. 3. DQ-decoupled control is adopted with limiters to restrict the output voltage. The system can be described by the

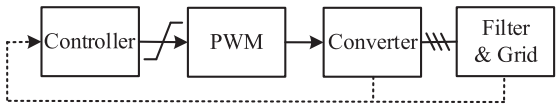

Fig. 4. Equivalent block diagram of the system.

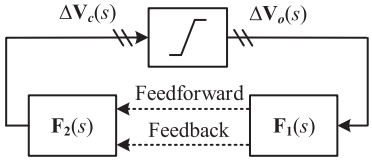

Fig. 5 Transfer function block diagram of the system.

TABLE I
CALCULATION RESULTS OF OSCILLATION FREQUENCY

Case	Eigenvalue	Simulation	Traditional	Improved
1	148.0Hz	145.6Hz	146.2Hz	145.8Hz
2	159.1Hz	154.3Hz	155.6Hz	154.4Hz
3	179.1Hz	169.3Hz	171.2Hz	169.4Hz

block diagram in Fig. 4. For slight sustained oscillations, the grid and the controller could be linearized near the equilibrium point. Therefore, the transfer function block diagram is shown in Fig. 5, in which the oscillation component in the output of VSC is $\Delta\mathbf{V}_o$, $\mathbf{F_1}(s)$ and $\mathbf{F_2}(s)$ represent the grid and the controller respectively. So, the linearized part of the system can be denoted as $\mathbf{F}(s) = \mathbf{F_1}(s)\mathbf{F_2}(s)$. The output voltage of the controller is $\Delta\mathbf{V}_c$, and when $\Delta\mathbf{V}_c$ goes through the limiter, $\Delta\mathbf{V}_o$ appears. Because the oscillation is sustained, we have $L(\Delta\mathbf{V}_c) = \Delta\mathbf{V}_o$, where the limiter is represented as L.

The model of VSC is usually established in dq-domain, so the closed-loop model of the system is

$$L\left(\begin{bmatrix} F_{dd}(s) & F_{dq}(s) \\ F_{qd}(s) & F_{qq}(s) \end{bmatrix}\begin{bmatrix} \Delta V_{od}(s) \\ \Delta V_{oq}(s) \end{bmatrix}\right) = \begin{bmatrix} \Delta V_{od}(s) \\ \Delta V_{oq}(s) \end{bmatrix} \tag{8}$$

If only d-axis limitation works under certain condition, there will be $\Delta V_{cq} = \Delta V_{oq}$. Hence, there is

$$L\left(\left[F_{dd}(s) + \frac{F_{dq}(s)F_{qd}(s)}{1 - F_{qq}(s)}\right]\Delta V_{od}(s)\right) = \Delta V_{od}(s) \tag{9}$$

Equation (9) can be simplified as

$$L\left(F_D(s)\Delta V_{od}(s)\right) = \Delta V_{od}(s) \tag{10}$$

Under the conditions of sustained oscillation, both the input and output of the limiter contain 1st∼3rd order components. As mentioned in Section II, the influence of the limiter can be described as three variable gains, N_1', N_2', and N_3', and these gains are determined by the 1st∼3rd order input components. In the linearized part, these three components are independent. So equation (10) can be further derived as (11) shown at the bottom of this next page, where ω_s is the angular frequency of 1st order component in dq-domain.

$$\begin{cases} N_1'(A, A_2, A_3, \alpha_2, \alpha_3)F_D(j\omega_s)\Delta V_{od1}(j\omega_s) \\ = \Delta V_{od1}(j\omega_s) \\ N_2'(A, A_2, A_3, \alpha_2, \alpha_3)F_D(j2\omega_s)\Delta V_{od2}(j2\omega_s) \\ = \Delta V_{od2}(j2\omega_s) \\ N_3'(A, A_2, A_3, \alpha_2, \alpha_3)F_D(j3\omega_s)\Delta V_{od3}(j3\omega_s) \\ = \Delta V_{od3}(j3\omega_s) \end{cases} \tag{11}$$

Equation (11) could be finally simplified into (12), which are complex equations. Hence the six unknowns A, A_2, A_3, α_2, α_3 and ω_s could be solved.

$$\begin{cases} N_1'(A, A_2, A_3, \alpha_2, \alpha_3)F_D(j\omega_s) = 1 \\ N_2'(A, A_2, A_3, \alpha_2, \alpha_3)F_D(j2\omega_s) = 1 \\ N_3'(A, A_2, A_3, \alpha_2, \alpha_3)F_D(j3\omega_s) = 1 \end{cases} \tag{12}$$

TABLE II
CALCULATION RESULTS OF OSCILLATION AMPLITUDE

Case	Order	Frequency	Amplitude of the output current (Unit: A)		
			Simulation	Traditional	Improved
1	1	f_0+f_s	2.20	2.28	2.33
		$\lvert f_0-f_s\rvert$	133	124	131
	2	f_0+2f_s	0.650	/	0.629
		$\lvert f_0-2f_s\rvert$	0.973	/	1.00
	3	f_0+3f_s	2.27	/	2.17
		$\lvert f_0-3f_s\rvert$	0.720	/	0.677
2	1	f_0+f_s	7.81	5.81	7.87
		$\lvert f_0-f_s\rvert$	148	131	147
	2	f_0+2f_s	1.90	/	1.95
		$\lvert f_0-2f_s\rvert$	1.55	/	1.65
	3	f_0+3f_s	4.00	/	4.28
		$\lvert f_0-3f_s\rvert$	1.44	/	1.49
3	1	f_0+f_s	27.1	18.4	26.6
		$\lvert f_0-f_s\rvert$	199	160	196
	2	f_0+2f_s	6.65	/	6.63
		$\lvert f_0-2f_s\rvert$	1.77	/	1.82
	3	f_0+3f_s	4.24	/	5.11
		$\lvert f_0-3f_s\rvert$	1.74	/	2.02

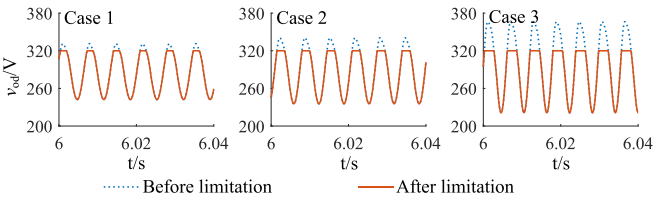

Fig. 6. Oscillations with different degree of limitation.

IV. CASE STUDIES

The system in Fig. 3 is established in PSCAD/EMTDC. Cases of different limitation degree shown in Fig. 6 are studied and the results are presented in TABLE I and TABLE II. TABLE I shows the 1st order frequencies in dq-domain. The eigenvalue analysis deviates the most from the practical oscillation frequency for the limitation could not be modeled in eigenvalue analysis. The k^{th} order oscillation with frequency kf_s in dq-domain could be

transformed to $f_0 \pm kf_s$ components in *abc*-domain. So when 1st∼3rd order components are considered, the output *A*-phase current of VSC contains six components, as shown in TABLE II. Compared with the traditional method, the improved one is more accurate, which becomes more obvious under severe limitation degree.

V. Conclusion

This letter proposes an analysis method for sustained oscillations, which considers high-order components. The high-order components could lead to phase shift in the 1st order output of the limiter, which would influence the frequency and amplitude of the sustained oscillations. Compared to the existing method, the proposed method could obtain more precise oscillation frequency and the amplitude of 1st∼3rd order components. It is revealed that when severe oscillation happens, high-order components have more impact on the accuracy of the calculation. The proposed method could also be extended to dual-axis limitation conditions and higher-order components. Under the conditions of dual-axis limitation, both *d*-axis limiter and *q*-axis limiter should be modeled. When higher-order components are considered, the accuracy of the calculation could be improved but the computation complexity will increase. Hence, a compromise between the precision and complexity should be reached according to the practical application scenarios.

References

[1] X. Wang, L. Harnefors, and F. Blaabjerg, "Unified impedance model of grid-connected voltage-source converters," *IEEE Trans. Power Electron.*, vol. 33, no. 2, pp. 1775–1787, Feb. 2018.

[2] Y. Xu, Z. Gu, and K. Sun, "Characterization of subsynchronous oscillation with wind farms using describing function and generalized nyquist criterion," *IEEE Trans. Power Syst.*, vol. 35, no. 4, pp. 2783–2793, Jul. 2020.

[3] T. Wu, Q. Jiang, J. Shair, H. Mao, and X. Xie, "Inclusion of current limiter nonlinearity in the characteristic analysis of sustained subsynchronous oscillations in grid-connected PMSGs," *IEEE Trans. Energy Convers.*, vol. 36, no. 3, pp. 2416–2426, Sep. 2020.

[4] T. Bi, J. Li, P. Zhang, E. Mitchell-Colgan, and S. Xiao, "Study on response characteristics of grid-side converter controller of PMSG to subsynchronous frequency component," *IET Renewable Power Gener.*, vol. 11, no. 7, pp. 966–972, 2017.

[5] Y. Wang, L. Wang, and Q. Jiang, "Frequency coupling characteristics of electromagnetic oscillation in grid-connected converters," *IET Gener., Transmiss. Distrib.*, vol. 13, no. 19, pp. 4339–4346, 2019.